Regenerative Therapy 30 (2025) 63–74

Contents lists available at ScienceDirect

Regenerative Therapy

journal homepage: http://www.elsevier.com/locate/reth

Original Article

A temperature-sensitive chitosan hydrogels loaded with nano-zinc oxide and exosomes from human umbilical vein endothelial cells accelerates wound healing

Lei Yu [a], Zihao Dai [a], Yuchen Huang [a], Shuo Tang [a], Lihong Zhou [c], Xuying Zhao [a], Xianfeng Que [e], Rongfeng Shi [f], Jin Zhou [b], Jixuan Dong [d], Feng Wang [b, **], Yunjuan Gu [a, *]

[a] Department of Endocrinology, Affiliated Hospital of Nantong University, Nantong University, 20 Xisi Road, Nantong, Jiangsu 226001, People's Republic of China
[b] Nantong Xingzhong Cell Engineering Co. LTD, Nantong, Jiangsu 226001, People's Republic of China
[c] Department of Histology and Embryology, Medical School, Nantong University, Nantong, Jiangsu 226001, People's Republic of China
[d] Department of Radiation Oncology, Affiliated Hospital of Nantong University, Nantong University, 20 Xisi Road, Nantong, Jiangsu 226001, People's Republic of China
[e] Health Management Center, Affiliated Hospital of Nantong University, Nantong University, 20 Xisi Road, Nantong, Jiangsu 226001, People's Republic of China
[f] Department of Interventional and Vascular Surgery, Affiliated Hospital of Nantong University, Nantong University, 20 Xisi Road, Nantong, Jiangsu 226001, People's Republic of China

ARTICLE INFO

Article history:
Received 8 January 2025
Received in revised form
15 April 2025
Accepted 24 April 2025

Keywords:
Exosomes
HUVECs
Diabetic wound healing
Chitosan based hydrogel
Skin regeneration

ABSTRACT

The suboptimal therapeutic outcomes of diabetic foot ulcers (DFUs) represent a significant global challenge. In recent years, studies have indicated that novel dressings incorporating exosomes (Exos), nanomaterials, and hydrogels following debridement can synergistically promote tissue repair, which has been widely recognized as a promising emerging trend in the treatment of DFUs. In this study, a combination of zinc oxide nanoparticles (ZnO-NPs), Exos, and chitosan (CS) hydrogel (CS/ZnO-NPs@Exos) was applied to the full-thickness cutaneous defects in a diabetic rat model. This CS/ZnO-NPs@Exos hydrogel was applied to the wound site to achieve sustained and long-term release of Exos, allowing the evaluation of its therapeutic effects. This hydrogel significantly improved the wound closure rate in diabetic skin injuries and reduced oedema, erythema and inflammatory exudate at the wound site. These effects were characterized by enhanced re-epithelialization, reduced infiltration of inflammatory cells, increased collagen deposition, and enhanced angiogenesis in the wound area. This may be related to the Exos derived from human umbilical vein endothelial cells (HUVECs), which notably promote the migration and proliferation of fibroblasts. As a result, the CS/ZnO-NPs@Exos hydrogel offers a new therapeutic dressing for the management of diabetic wounds, with the potential to play a crucial role in clinical practice.

1. Introduction

Diabetes mellitus is a chronic disease that is prevalent worldwide. Long-term hyperglycaemia due to diabetes can severely damage the vascular and nervous systems, leading to severe complications, including diabetic foot ulcers (DFUs) [1]. Recent data indicate that by 2025, the number of type 2 diabetes patients in China will exceed 130 million [2]. According to the American Diabetes Association, annual expenditures related to DFUs care in the United States amount to as much as $109 billion, which has

* Corresponding author.
** Corresponding author.
E-mail addresses: 15335050161@163.com (F. Wang), ntdxguyunjuan@163.com (Y. Gu).

Peer review under responsibility of the Japanese Society for Regenerative Medicine.

https://doi.org/10.1016/j.reth.2025.04.020

significantly strained societal and health care resources. Worldwide, a DFUs patient undergoes amputation every 20 s, indicating the severe burden this condition places on human health and quality of life. The mechanisms underlying the poor healing of DFUs are associated with factors such as hyperglycemia, neuropathy, microvascular complications, chronic inflammation, and impaired immune function [3,4]. Currently, there is no unified clinical treatment for DFUs, and the unsatisfactory outcomes of DFUs treatments present a major global arena. Thus, an in-depth exploration of DFUs treatment modalities is of great clinical significance.

At present, on the basis of systemic treatment, current therapeutic strategies for DFUs predominantly focus on local treatment, which has remained a challenge in recent years [5]. Local treatment methods include debridement, the application of biological dressings, vascular reconstruction and medical maggot therapy. Dressing application is a key part of DFUs management. The primary objective for both patients and health care providers is to aid in wound healing by applying innovative dressings following debridement. An optimal wound dressing should possess attributes such as ease of application, patient comfort, cost efficiency, and the ability to maintain a moist wound environment. Furthermore, the dressing should inhibit secondary infections and facilitate tissue regeneration. Extensive research has demonstrated the great efficacy of biomaterial composites in promoting wound healing. It has been reported that dressings composed of biomaterials such as hydrogels, nanomaterials, chitosan (CS), and exosomes (Exos) can synergistically enhance tissue repair; thus, such dressings have garnered considerable attention for their potential applications in wound closure [6]. Combinations of Exos and biomaterials have been reported to synergistically promote tissue repair, which has led to a great emphasis being placed on the use of Exos in wound closure [7]. Moreover, hydrogels not only preserve the inherent biological functionality and activity of Exos but also extend the retention time of Exos at the wound site. The local application of Exos has been found to be more effective than subcutaneous administration [8]. A growing number of studies have demonstrated that Exos loaded within hydrogels can significantly accelerate wound healing [9,10].Consequently, hydrogel-loaded Exos hold great promise as a therapeutic approach for the treatment of DFUs.

Exos are nanovesicles with a diameter of 30–150 nm that are derived from endosomal structures [11]. Exos are believed to be closely involved with paracrine effects and can induce tissue repair capabilities that are equal to or greater than those of their source cells [12]. Exos regulate intercellular communication by transferring RNA or proteins to target cells. They play a crucial role in various biological processes, including tissue damage, infection, immune response, and healing [13,14]. The Exos studied in this study are derived from HUVECs (H-Exos), which offer several advantages, including an abundant source, ease of isolation, strong proliferative capacity, low immunogenicity, and the absence of ethical concerns. The blood in the umbilical vein is typically arterial blood, which is rich in oxygen and nutrients. This blood contains a variety of cytokines and growth factors, which can regulate vascular dilation and contraction, as well as platelet aggregation [15,16]. Surprisingly, H-Exos could accelerate wound healing [17]. Gelatin methacryloyl (GelMA) hydrogel is a visible light crosslinked biomaterial with adjustable properties. Researchers use it to create three-dimensional constructs containing cells or factors, which can be sustainably released after incorporating H-Exos. The continuous release of GelMA wound dressing through H-Exos can not only serve as a scaffold for repairing wound defects, but also promote angiogenesis and skin regeneration during wound healing. GelMA hydrogel mediated controlled release of H-Exos offered a new method for repairing cutaneous wound defects. However, DFUs are often accompanied by local infections [18], while GelMA hydrogels appear to lack inherent antibacterial properties. Therefore, hydrogels with antibacterial functionalities continue to hold significant research value in this field.

The application of CS as a wound dressing aims to achieve a sustained release function through the encapsulation of Exos [19]. Furthermore, existing studies have demonstrated that CS exhibits multiple biological activities, including analgesic effects, anticoagulant properties, antimicrobial and preservative functions, as well as the promotion of angiogenesis [20,21]. Zinc oxide nanoparticles (ZnO-NPs), novel inorganic nanomaterials, possess outstanding antimicrobial properties, long-lasting antibacterial effects, and excellent biocompatibility [22]. Composite hydrogels prepared by combining CS with nanomaterials have the advantages of improved thermal stability, antimicrobial activity, and mechanical tensile strength. Interestingly, it was reported in that composite hydrogels prepared with both ZnO-NPs and CS displayed greater inhibition of free bacteria and greatly improved the antimicrobial activity of CS gels, which may be related to the ability of ZnO-NPs to disrupt the bacterial cell wall more effectively [23]. In conclusion, the combination of CS/ZnO-NPs composite hydrogels and Exos can avoid the loss of these biomolecules for their application and greatly promote wound healing. We hypothesize that the Exos sustained-release system composed of CS/ZnO-NPs, in combination with the functional properties of H-Exos, can not only jointly promote wound healing and skin regeneration but also alleviate pain or secondary infections in DFUs. This approach may provide a novel perspective for the treatment of DFUs.

On the basis of the aforementioned research, we integrated CS/ZnO-NPs composite hydrogels with H-Exos to create a composite gel. This gel was subsequently applied to diabetic ulcers to evaluate its therapeutic efficacy. The in vivo results confirmed that CS/ZnO-NPs@Exos effectively shortened the diabetic wound healing time and increased vascularization and collagen deposition at the wound site. Collectively, our findings demonstrate the clinical potential of the CS/ZnO-NPs@Exos hydrogel in healing DFUs.

2. Materials and methods

2.1. Materials

CS (MW, degree of deacetylation ≥95 %) was purchased from Aladdin Biochemical Technology Co., Ltd. (Shanghai, China); ZnO-NPs and β-glycerophosphate were obtained from Maclean Biochemical (China); and Dulbecco's modified Eagle's medium (DMEM) and foetal bovine serum (FBS) were obtained from Gibco Technologies. All other chemicals were of analytical grade and purchased from various vendors.

2.2. Cells and cell culture

Human foreskin fibroblasts (HFF-1 cells, American Type Culture Collection) and HUVECs (Wuhan Servicebio Technology, China) were cultured in low-glucose DMEM (Gibco, Grand Island, New York, USA) supplemented with 10 % FBS (Gibco, Grand Island, New York, USA) and complete medium supplemented with 1 % PS (Gibco, Grand Island, New York, USA) in a humidified atmosphere containing 5 % CO_2 at 37 °C.

2.3. Isolation and identification of the Exos

H-Exos culture medium supernatant via size-exclusion chromatography and ultracentrifugation. First, a chromatography column filled with porous gel particles was used for size-exclusion chromatography. Second, the mixture was centrifuged at 300×*g* for

10 min, 2000×*g* for 10 min and 10,000×*g* for 30 min to remove cells and cell debris and then filtered through a 0.22 μm filter (Millipore, Massachusetts, USA) with centrifugation at 100,000×*g* for 70 min. The supernatant was subsequently discarded, and the Exos were resuspended in phosphate-buffered saline (PBS) and centrifuged at 100,000×*g* for 70 min to wash the pellet. All steps were performed at 4 °C. The isolated Exos were resuspended in PBS and stored at −80 °C for subsequent identification and experiments.

Transmission electron microscopy (TEM; JSM-4800, Hitachi, Japan) and Western blotting were used to identify the characteristics of the H-Exos. The size distribution and concentration of Exos were analy confirming the high preparation purity without endoplasmic

zed using nanoparticle tracking analysis (NTA; Malvern Instruments, UK). Protein quantification was subsequently performed using a BCA protein assay kit (Thermo Fisher Scientific, Grand Island, New York), followed by Western blot.

2.4. Exos uptake by HFF-1 cells

To examine the internalization of H-Exos by HFF-1 cells, Exos were labeled with the red fluorescent dye PKH26 (Umibio Bio, Shanghai, China). According to the manufacturer's instructions, ultracentrifugation (100,000×*g*, 70 min) was performed to remove the excess dye [24]. The PKH26-labeled Exos were resuspended in 1 mL of PBS. Subsequently, PKH26-labeled Exos locally applied to the wound site of diabetic rats after a 48-h period, skin tissue samples from the wound area were collected for further analysis. HFF-1 cells were seeded in a 24-well plate. When the cells reached 80 % confluence, they were treated with PKH26-labeled Exos and incubated for 24 h. The cells were subsequently fixed in 4 % paraformaldehyde for 15 min and washed with PBS. The uptake of PKH26-labeled Exos by HFF-1 cells was determined via confocal laser scanning microscopy.

2.5. Scratch assay

Cell migration was assessed via a scratch assay. HFF-1 cells were seeded at a density of 1×10^5 cells/mL in 6-well plates and allowed to reach approximately 95 % confluence [25]. In each well, four parallel scratches were created with a 200 μL pipette tip. Dislodged cells and debris were removed by washing with phosphate-buffered saline. The cells were subsequently subjected to various treatments, including 10 μg/μL Exos, or left untreated (control conditions). The cells were then incubated for 0, 4, 12, or 24 h. The width of the scratch was visually observed via a light microscope (Leica, Germany) and measured with ImageJ software.

2.6. Preparation and characterization of thermosensitive hydrogels

Two hundred milligrams of CS was weighed at room temperature and dissolved in 10 mL of 0.1 mol/L acetic acid solution. Subsequently, 6 mg of ZnO-NPs was added, and the mixture was subjected to ultrasonication for 1 min. Approximately 4.24 g of β-Glycerophosphate (β-GP) was weighed and dissolved in 5 mL of deionized water. The ZnO-NPs/CS and 56 % (w/v) β-GP were mixed at a ratio of 7:3 with continuous magnetic stirring in an ice water bath. The CS/ZnO-NPs@Exos hydrogels were prepared by mixing H-Exos and CS/ZnO-NPs at a ratio of 1:3. The chemical structure of the hydrogel was analysed via Fourier transform infrared (FTIR) spectroscopy (Thermo Nicolet Corp, USA).

PKH26 fluorescent labeling was employed to systematically investigate the distribution characteristics of Exos within the CS/ZnO-NPs@Exos composite hydrogel, with visualization analysis performed using confocal laser scanning microscopy. A control group (hydrogel containing 50 μl PBS) was established for parallel observation. To examine the release profile of Exos from the CS/ZnO-NPs@Exos hydrogel, 100 μL of the hydrogel was loaded into the upper chamber of a 24-well plate [26]. Following gelation, 1200 μL of PBS was added to the lower chamber, and the system was maintained at 37 °C. At predetermined time intervals, 400 μL samples were collected and replaced with an equal volume of fresh PBS. Exos release was quantified using a Micro BCA Protein Assay Kit (Zeye Biotechnology, China). The cumulative release profile was plotted based on these measurements.

2.7. Cytotoxicity of the exos loaded within the CS/ZnO-NPs hydrogel

MTT assays were performed to assess whether the CS/ZnO-NPs hydrogel loaded with H-Exos could enhance the proliferation of HFF-1 cells or exhibited toxicity in vitro. The CS/ZnO-NPs hydrogel was immersed in an equal volume of DMEM supplemented with 10 % foetal bovine serum (FBS) and incubated in a 37 °C incubator to generate the hydrogel extraction solution. After 24 h of routine cell culture, the medium was aspirated, and the hydrogel extraction solution was added to the cells for 36 h of culture. The cells attached to the hydrogels or well plates were treated with thiazolyl blue (MTT; 5 mg/mL in PBS, Maclean). After 4 h, the purple MTT formazan crystals were dissolved by adding 200 μL of 10 % SDS. After standing for 12 h, the absorbance of each sample was measured at 570 nm.

2.8. Diabetic wound healing model

The animal study was approved by the Animal Research Committee of Nantong University School of Medicine. Sprague–Dawley (SD) rats (male, 200 ± 20 g, 8–10 weeks) were provided by the laboratory Animal Center of Nantong University. All the rats were fed in a room with a 12-h light/dark cycle at a stable temperature (25 °C) and humidity. Streptozotocin (STZ; 65 mg/kg, Sigma, USA) was dissolved in citrate-sodium citrate buffer and used to induce diabetes in the SD rats upon intraperitoneal injection. The blood glucose levels of the rats were measured beginning on Day 3 after injection, and the rats with blood glucose levels higher than 16.67 mmol/L for 3 consecutive days were considered the diabetes model rats. A model was then created for wound healing following STZ injection and induction of a 4-week diabetic state. After establishing anaesthesia via intraperitoneal injection with 3 % sodium pentobarbital, depilatory cream was applied to remove the dorsal hair, and a standard full-thickness wound was created by making a circular punch with a diameter of 15 mm [6,27]. The rats were randomly divided into 3 groups: the control group (PBS), the CS/ZnO-NPs hydrogel group, and the CS/ZnO-NPs@Exos hydrogel group. The wound sites in the CS/ZnO-NPs hydrogel group and the CS/ZnO-NPs@Exos hydrogel group were covered with 200 μL of the respective hydrogels. Next, the wound sites were covered with TegadermTM (3 M, USA). Postoperatively, the rats in each group were individually housed, and wound healing was observed. Changes in the sizes of the diabetic wounds were evaluated by taking photographs on Days 0, 3, 7, 10, and 14 after surgery. Wounds were washed with normal saline on Days 3, 7, and 10, after which fresh hydrogel or PBS was applied. On Day 14, the animals were sacrificed after the wound areas were washed with normal saline for further analysis. The wound healing rate was measured with ImageJ software (NIH, USA) and calculated via the following formula: wound closure rate = (S0-SA)/S0 × 100 %, where S0 represents the original wound area on Day 0, and SA represents the wound area on Day A.

2.9. Histopathological staining

Tissue samples were obtained from the damaged sites, and full-thickness wound tissue samples (approximately 20 mm each) were harvested along the outer edge of the entire wound [28]. The collected tissue samples were fixed overnight at 4 °C in 4 % paraformaldehyde, embedded in OCT, and used to prepare tissue sections (8 μm) on glass slides for histological analysis. Haematoxylin and eosin (H&E) and Masson's trichrome staining were used to determine the thickness of the newly formed epithelium and the deposition of collagen at the site of injury, respectively. Photographs were captured via a microscope and a digital camera (Zeiss, Germany).

2.10. CD31 immunohistochemistry and quantitation of microvessel density

Immunohistochemistry with a rabbit anti-rat CD31 antibody (Wuhan Servicebio Technology, China) was performed on tissue sections to assess angiogenesis in the wounds following intervention [29]. The samples were incubated overnight at 4 °C with the primary CD31 antibody. The sections were then incubated with an HRP-conjugated goat anti-rabbit secondary antibody (1:200, Servicebio) for 1 h. The binding of the antibodies to the tissue sections was visualized by incubation with DAB substrate. After counterstaining with haematoxylin, the CD31-stained blood vessels were observed under a microscope. Three areas with the highest density of newly formed blood vessels were selected at low magnification (5 ×) on each glass slide. Three random regions within each of these areas were subsequently imaged at 20 × magnification. These images were analysed with ImageJ Plus software.

2.11. Statistical analysis

All the data are presented as the means ± SDs. Statistical analysis of the data was performed via Student's *t*-test (two groups), one-way ANOVA or two-way ANOVA. These data were analysed with GraphPad Prism. A value of $P < 0.05$ was considered to indicate statistical significance.

3. Results

3.1. Characterization of the H-Exos

Using previously described methods, we successfully isolated Exos. Exos isolated from HUVECs were identified through particle size measurements, TEM, and Western blotting. TEM revealed that the H-Exos displayed typical saucer-like structures (Fig. 1A). NTA demonstrated an average particle size of approximately 100 nm (Fig. 1C) and an exosomal concentration of 1.9×10^8 particles/mL, which was in accordance with the shape and size reported in a previous study [30]. The Western blot results revealed that the H-Exos highly expressed the surface markers CD63 and TSG101, whereas calnexin was not expressed (Fig. 1B), confirming the high preparation purity without endoplasmic reticulum contamination.

3.2. H-Exos promote the migration of HFF-1 cells

Fibroblasts are among the key cells involved in wound healing; fibroblasts migrate from the surrounding tissue to the wound site, become activated, begin synthesizing collagen and proliferate [31,32]. Fibroblasts also further stimulate the migration and proliferation of keratinocytes at the edge of the wound so that the newly generated epidermis can completely cover the wound. To assess the uptake of Exos, HFF-1 cells were coincubated with PKH26-labeled Exos, followed by observation under a fluorescence microscope. Significant amounts of red fluorescent Exos were observed in the cytoplasm of HFF-1 cells, confirming that H-Exos can be internalized by HFF-1 cells (Fig. 2A). In this study, the wound healing rates were determined via an in vitro scratch assay. All the cells were cultured in complete medium supplemented with 2 % FBS to eliminate the serum-mediated promotion of cell proliferation. Within 24 h of culture, compared with the control group, the cells in the Exos-treated group maintained their elongated spindle shapes with clear boundaries, and no significant morphological changes were observed (Fig. 2B). Furthermore, at various time points, HUVECs treated with H-Exos exhibited significantly enhanced cell migration and proliferation. Compared with that in the control group, the cell-free area in the Exos-treated group was reduced by 17.4 % at 4 h, 31.4 % at 12 h, and 45.7 % at 24 h (Fig. 2B and C).

3.3. Properties of the CS/ZnO-NPs hydrogel

This hydrogel, prepared at room temperature, can rapidly gel at 37 °C in a constant-temperature water bath, which demonstrates its excellent temperature sensitivity (Fig. 3A). FTIR analysis of the CS/ZnO-NPs hydrogel was performed to determine the chemical structure of the hydrogel (Fig. 3B). Changes in the absorption peaks and stretching vibrations of ZnO-NPs/CS/β-GP were analysed. The ZnO-NPs presented characteristic absorption peaks at 475 cm−1, which corresponds to the tensile vibrations of Zn−O, and at 3346 cm−1 and 1635 cm−1, which correspond to the stretching vibrations of O−H and are associated with the uptake of water by the ZnO-NPs from the air. In the CS and ZnO-NPs infrared spectra, the absorption peak at 3305 cm-1 was attributed to the combined vibrations of O−H and N−H bonds, whereas the peaks at 2937, 1558, and 1115 cm-1 corresponded to C−H tensile vibrations, N−H bending vibrations, and O−H tensile vibrations, respectively. The strengthened forces due to intermolecular hydrogen bonding in the composite hydrogels contributed to the formation of a dense composite hydrogel [33]. Moreover, no significant new absorption peaks were observed in the spectrum of the composite hydrogel, indicating that the ZnO-NPs did not significantly affect the structure of the composite hydrogel, which is consistent with previous reports [23].

One important criterion for evaluating the quality of biomaterials is their biocompatibility. The biocompatibilities of the CS/ZnO-NPs hydrogels alone and that upon incorporation into Exos were evaluated via cell culture experiments with HFF-1 cells. Fig. 3C shows the shape of the HFF-1 cells cultured with the hydrogel extract. Cell proliferation on the hydrogel was quantitatively assessed with MTT assays. At 36 h, there was no difference in the absorbance values between the CS/ZnO-NPs hydrogel experimental group and the control group. The CS/ZnO-NPs hydrogel had no significant effect on HFF-1 cell proliferation. Furthermore, treatment with the CS/ZnO-NPs@Exos resulted in a rate of cell proliferation that was greater than those in the control group and the CS/ZnO-NPs hydrogel group, indicating that Exos in combination with the CS/ZnO-NPs hydrogel synergistically promoted cell proliferation (Fig. 3D). These results confirm that the CS/ZnO-NPs hydrogel is biocompatible and does not exhibit cytotoxicity.

PKH26-labeled H-Exos exhibited homogeneous distribution within the CS/ZnO-NPs hydrogel (Fig. 3E), demonstrating excellent dispersibility of Exos in the hydrogel, which is conducive to drug delivery safety. The release analysis (Fig. 3F) revealed that the CS/ZnO-NPs hydrogel displayed sustained Exos release characteristics: the release rate was 18.8 % in the first 12 h, 62.9 % by day 2, and reached 98.7 % by day 5. This release profile may be associated with the rotational speed of the constant-temperature shaker. These

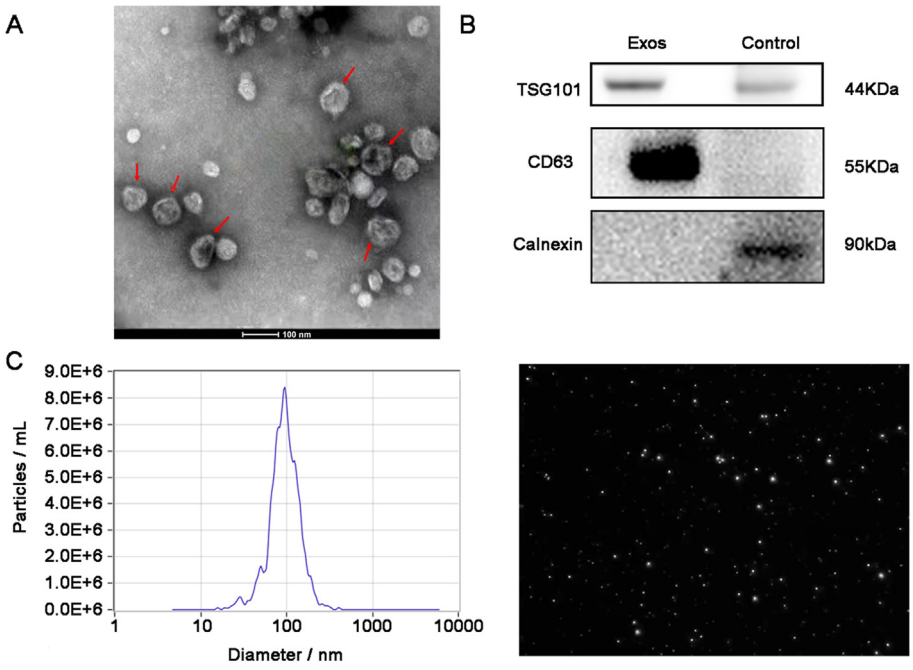

Fig. 1. Characterization and internalization of H-Exos. (A) The morphology of H-Exos observed by TEM. Scar bar = 100 nm. (B) Western blot detection of exosome markers CD63, TSG101 and negative control Calnexin. (C) Measurement of H-Exos population by NTA.

findings indicate that the CS/ZnO-NPs hydrogel effectively retains Exos at the local site, with subsequent release occurring progressively through hydrogel biodegradation, thereby enabling therapeutic efficacy.

In a diabetic rat model, PKH26-labeled H-Exos were topically applied to the wound site. 48 h later, the rats were euthanized, and skin tissue samples from the wound area were collected for analysis. Confocal microscopy results revealed that no red fluorescence signal was detected in the skin tissue sections of the control group (Fig. 3G). However, in the experimental group, the skin tissue sections (labeled with PKH26-labeled H-Exos) exhibited a prominent red fluorescence signal. These findings indicate that PKH26-labeled H-Exos can be effectively absorbed by the cells at the wound site. Collectively, these results demonstrate that the CS/ZnO-NPs@Exos system achieves effective Exos release, and the released Exos are successfully internalized by wound cells, thereby enhancing therapeutic outcomes.

3.4. CS/ZnO-NPs@Exos accelerate wound healing in diabetic rats

We next compared the healing efficiency of the CS/ZnO-NPs hydrogel and CS/ZnO-NPs@Exos hydrogel during the cutaneous wound repair process in a diabetic rat model. Fig. 4A shows representative images of the wound areas in each group treated with PBS (as a negative control), the CS/ZnO-NPs hydrogel, and the CS/ZnO-NPs@Exos hydrogel at Days 0, 3, 7, 10, and 14. The results indicated that, compared to the control group, the CS/ZnO-NPs hydrogel group exhibited faster wound healing, with a significant reduction in erythema, oedema, and inflammatory exudate at the wound site. No obvious signs of infection were observed. Furthermore, diabetic rats treated with the CS/ZnO-NPs@Exos hydrogel not only showed a marked reduction in erythema and oedema around the wound, but also demonstrated accelerated granulation tissue formation. On the third day, the wound healing rate in the control group was 24.9 %, while the rates in the CS/ZnO-NPs and CS/ZnO-NPs@Exos groups reached 38.5 % and 49.2 %, respectively (Fig. 4B). Compared with the control group, the CS/ZnO-NPs hydrogel and CS/ZnO-NPs@Exos hydrogel groups both exhibited significantly accelerated wound healing. By the seventh day, this difference in healing became more pronounced. The CS/ZnO-NPs@Exos hydrogel demonstrated the highest wound healing rate of 75.5 %, surpassing both the control group and the CS/ZnO-NPs group. Overall, CS/ZnO-NPs@Exos treatment had the best therapeutic effect, which may be attributed to the biological activity of the incorporated Exos.

Reducing scar width and increasing collagen deposition are parameters used to assess the degree of wound closure. H&E staining is an important indicator for assessing the healing pathology of wounds treated with the CS/ZnO-NPs-Exos hydrogel. As shown in Fig. 4C, no neoepidermis had formed by Day 14 in the control group, but abundant granulation tissue had formed at the wound sites in the CS/ZnO-NPs and CS/ZnO-NPs@Exos hydrogel groups. The re-epithelialization rate for the CS/ZnO-NPs group was 68.8 %, compared with 53.4 % in the control group, and the CS/ZnO-NPs@Exos hydrogel group displayed the highest re-epithelialization rate of 90.9 % (Fig. 4D). In addition, skin appendages were clearly observed in the CS/ZnO-NPs@Exos hydrogel group showed that the prolonged release of Exos from the CS/ZnO-NPs@Exos hydrogel efficiently aided in the repair and regeneration of diabetic wounds. Collagen deposition and remodeling can increase the tensile strength of tissue, provide tension for skin and scar tissue, and lead to improved wound repair effects. Masson staining revealed significantly more collagen deposition in wounds treated with the CS/ZnO-NPs@Exos hydrogel than in the other wounds (the control and CS/ZnO-NPs hydrogel groups), with a deposition rate of 79.1 % (Fig. 4E and F). These data suggest that H-Exos treatment accelerates the process of diabetic wound repair in rats.

3.5. H-Exos enhance angiogenesis at the wound site

Angiogenesis is considered to play a critical role in tissue regeneration, as it facilitates the delivery of nutrients, oxygen, and growth factors to the wound area, thereby promoting cell proliferation, re-epithelialization, and collagen synthesis. Therefore, we

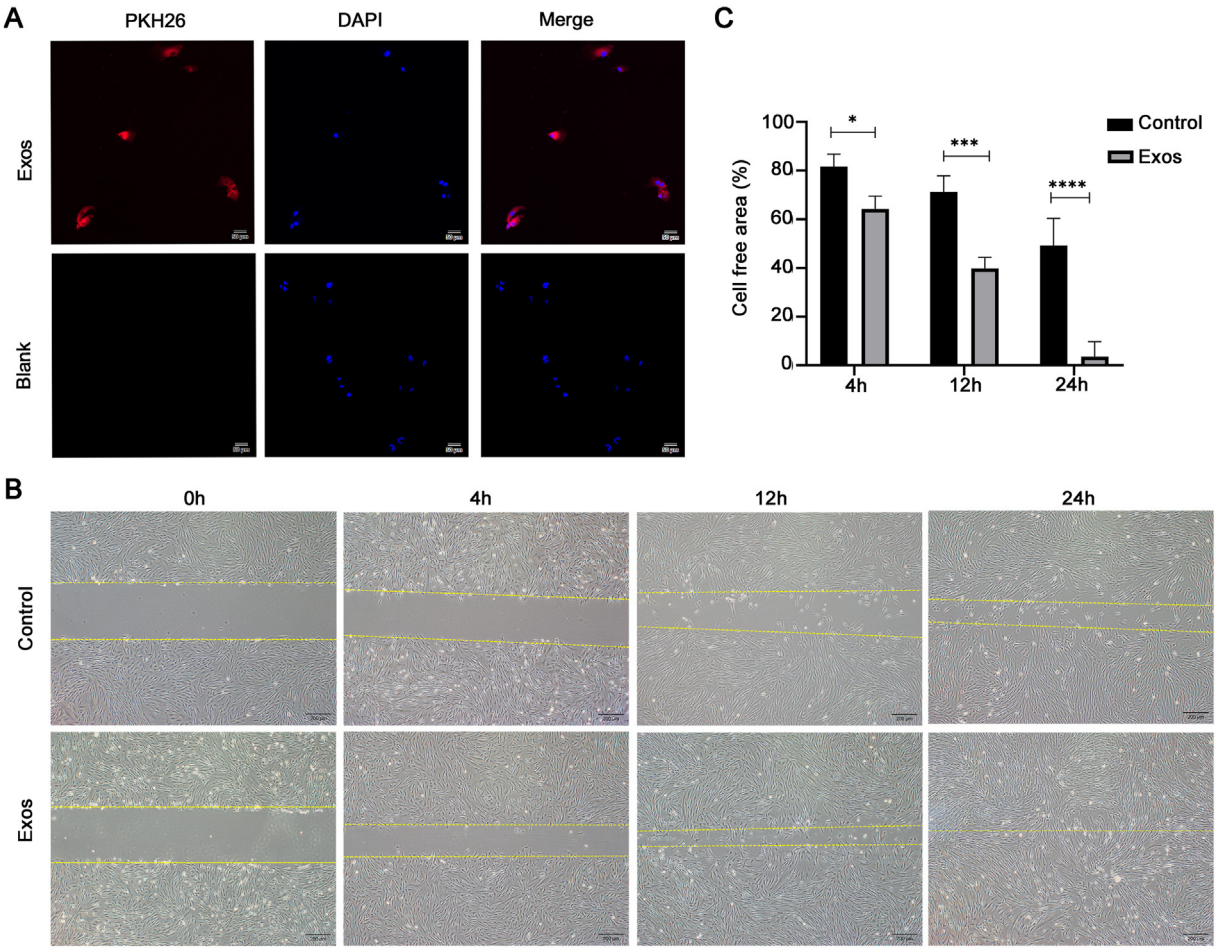

Fig. 2. Representative images of the scratch migration assay of HFF-1. (A) Immunofluorescence staining showing PKH26-labeled H-Exos (red) in HFF-1 cells. Nuclei stained blue by DAPI. Scale bar, 50 μm. (B) Migration states for control (culture medium), and H-Exos. (scale bar = 200 μm). (C) Quantitative analysis of scratch assays (n = 3, $^{*}P < 0.05$, $^{***}P < 0.001$, $^{****}P < 0.0001$).

assessed the newly formed microvasculature in the granulation tissue via immunohistochemical staining of tissue sections with antibodies targeting the endothelial cell marker CD31. On day 14 post-treatment, the control group exhibited the lowest number of CD31-positive blood vessels among all groups (Fig. 5A). Quantitative analysis revealed that the neovascularization density in the control group was only 37.91 ± 10.22 % (Fig. 5B), with predominantly immature cord-like structures and incomplete lumen formation. In contrast, the CS/ZnO-NPs hydrogel group showed significantly higher vascular density (61.60 ± 4.47 %) and improved morphological integrity. Most remarkably, the CS/ZnO-NPs@Exos hydrogel group demonstrated optimal pro-angiogenic effects, achieving 89.95 ± 8.07 % vascular density, with the majority of vessels displaying characteristic mature lumen structures. This well-developed vascular network could provide adequate oxygen and nutrient supply to the wound area, thereby significantly enhancing tissue regeneration. These findings confirm that the CS/ZnO-NPs@Exos composite hydrogel effectively accelerates diabetic wound healing by potentiating angiogenesis.

4. Discussion

The progresses of normal wound healing in skin through three interrelated and overlapping stages: haemostasis-inflammation, proliferation, and remodeling. In contrast, the wounds of DFUs exhibit significant deviations at multiple critical stages, hindering the occurrence of normal physiological healing responses and resulting in prolonged wound healing. In this study, we successfully isolated Exos derived from HUVECs and incorporated them into a composite hydrogel with CS and ZnO-NPs, thereby forming the composite gel CS/ZnO-NPs@Exos. The results predicted that CS/ZnO-NPs@Exos significantly inhibited wound inflammation and promoted re-epithelialization, collagen deposition, and angiogenesis in diabetic wounds in rats. Through multiple mechanisms, this composite hydrogel accelerated wound healing in diabetic ulcers, offering a promising new dressing for clinical application in DFUs.

Exos, as nano-sized extracellular vesicles, are critical bioactive molecules secreted by mesenchymal stem cells. These Exos promote wound healing by activating signaling pathways associated with tissue repair, including WNT, AKT, ERK, NF-κB, and STAT3, thereby facilitating cell proliferation and migration, modulating inflammation, enhancing collagen deposition at the wound site, and promoting angiogenesis [34–36]. Notably, Exos derived from different cell sources exhibit significant differences in their bioactive components and biological effects. Studies have shown that H-Exos display bioeffects similar to those of HUVECs in certain contexts [37]. Additionally, Li et al. discovered that Exos derived from hypoxia-preconditioned HUVECs significantly enhance the angiogenic potential of mesenchymal stem cells [38]. Other research indicates that H-Exos effectively ameliorate the photo-aging of skin

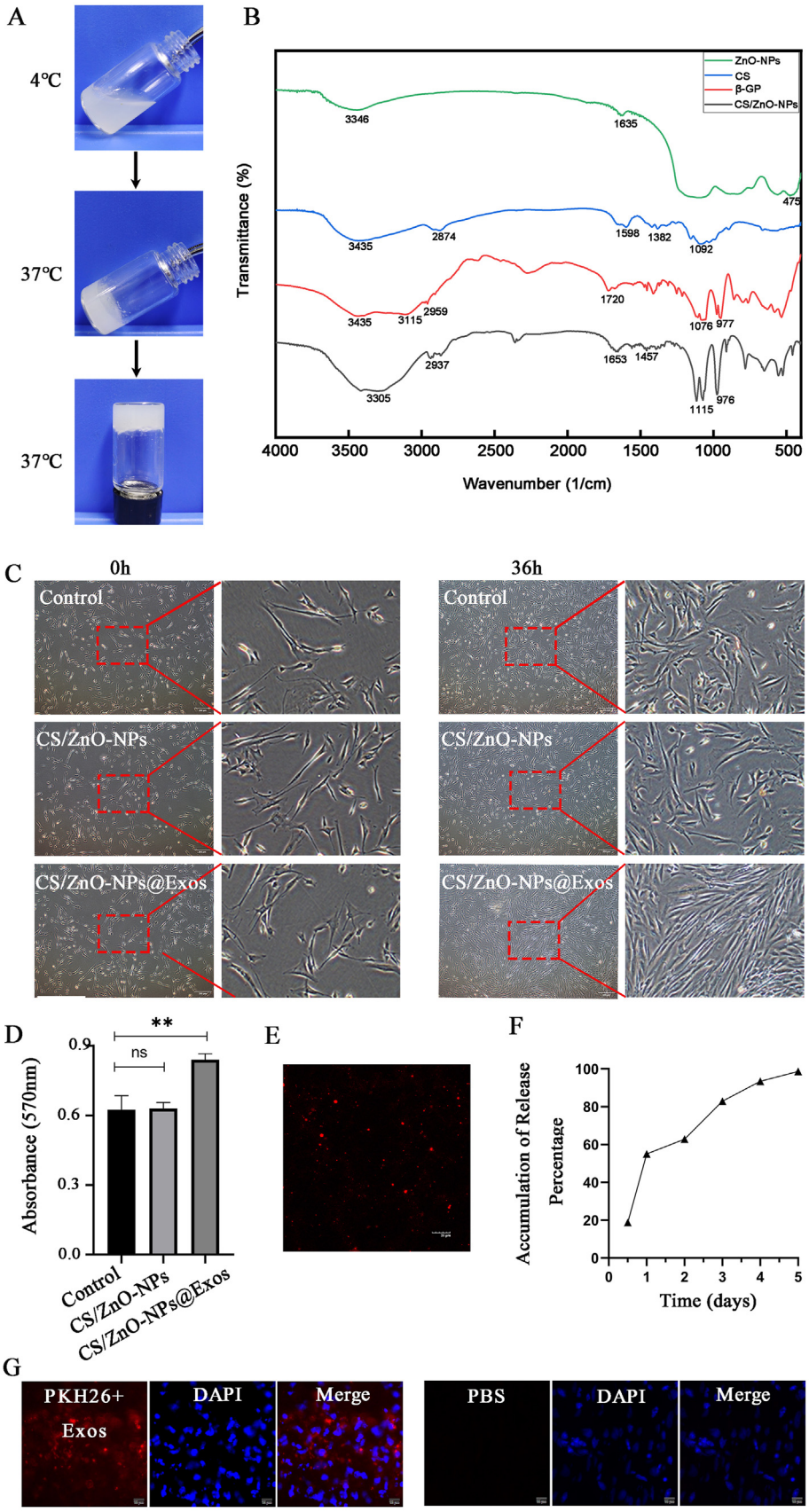

Fig. 3. The characterization of CS/ZnO-NPs hydrogel and H-Exos internalization by cells at the wound site. (A) Temperature sensitivity of hydrogels. (B) FTIR spectra of the CS, ZnO-NPs, β-GP and CS/ZnO-NPs hydrogel. (C) Shape of HFF-1 incubated for 36 h with hydrogel extract and hydrogel extract containing H-Exos (scale bar = 200 μm). (D) Cell proliferation rate was determined by MTT assay (N = 6), $^{**}P < 0.01$. (E) Dispersion characteristics of Exos in hydrogel (scale bar = 20 μm). (F) Release profile of loaded Exos in CS/ZnO-NPs@Exos hydrogel. (G) Immunofluorescence staining showing PKH26-labeled Exos (red) in skin tissue of diabetic rat. Nuclei stained blue by DAPI. Scale bar, 50 μm.

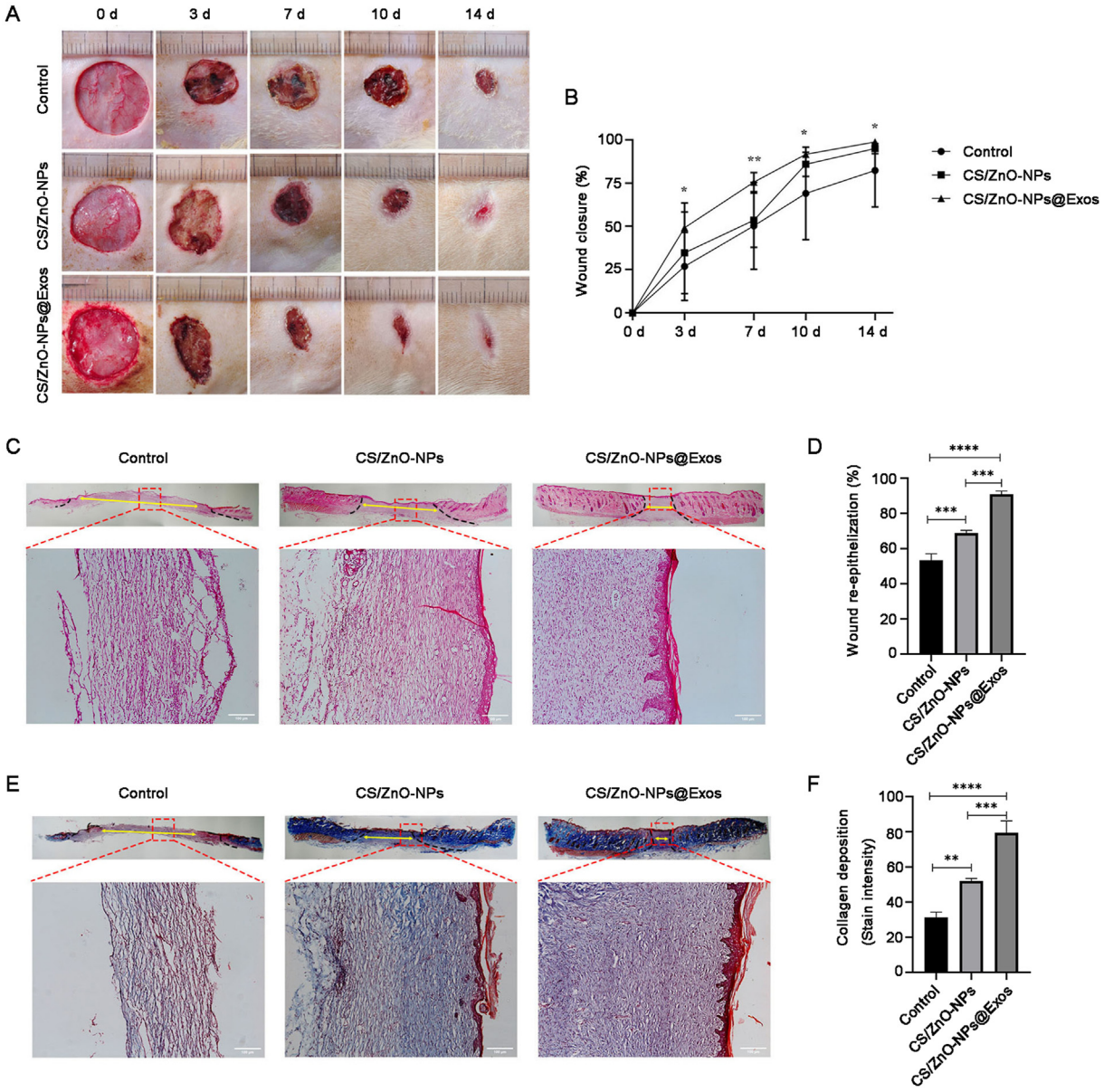

Fig. 4. Promotion of cutaneous wound healing by CS/ZnO-NPs hydrogels (with and without H-Exos) in a diabetic rat model. (A) The representative images of full-thickness cutaneous defects on days 0, 3,7, and 14 of the control group, CS/ZnO-NPs hydrogels and CS/ZnO-NPs hydrogels loaded with H-Exos after surgery. (B) The rate of wound-closure (%) quantitative analysis of all groups (n = 6 per group). (C) The images of H&E staining of the wound section in each group at 14 days post-wounding. The yellow arrows indicate the length un-epithelialization in the damaged sites. Scale bar, 100 μm. (D) Quantitative analysis of wound re-epithelialization shown in C. (E) Representative images of Masson's trichrome staining of the wound section in each group at 14 days after surgery. Scale bar, 100 μm. (F) Image J software was used to measure the collagen deposition of blue collagen shown in E. *$P < 0.05$, **$P < 0.01$, ***$P < 0.001$, ****$P < 0.0001$.

fibroblast [39]. These findings provide substantial evidence for the potential application of H-Exos in the promotion of wound healing, particularly in the context of diabetic ulcer repair.

Exos extraction methods are diverse; however, the Exos obtained by different techniques exhibit variations in terms of yield, purity, and activity, each with its respective advantages and disadvantages. In contrast to the approach employed by Zhao et al. [17], which utilizes a combination of ultrafiltration and ultracentrifugation to isolate H-Exos, the present study adopts a strategy combining ultracentrifugation and size-exclusion chromatography for Exos separation [17,40,41]. This method offers notable advantages, including lower impurity content, higher purity, stable separation efficiency, and enhanced reproducibility. The results indicate that the isolated Exos exhibit typical structural characteristics, high expression of Exos surface markers, and a particle size consistent with previous literature reports (Fig. 1A–C). Furthermore, the concentration of the Exos was determined to be 1.9×10^8 particles/mL. These results suggest that the methodology employed in this study is reliable and feasible for Exos isolation, providing high-quality samples for subsequent functional research.

Exos can exert their biological functions through cell membrane fusion with the target cell, thereby potentially impacting the functional phenotype of the recipient cells [42]. Research has shown that during the proliferative phase (Day 4 through 14) or remodeling phase (Day 8 through Year 1) of wound healing, fibroblasts migrate to the wound site and become activated [43]. These fibroblasts are primarily responsible for the synthesis and secretion of extracellular matrix components, such as collagen and

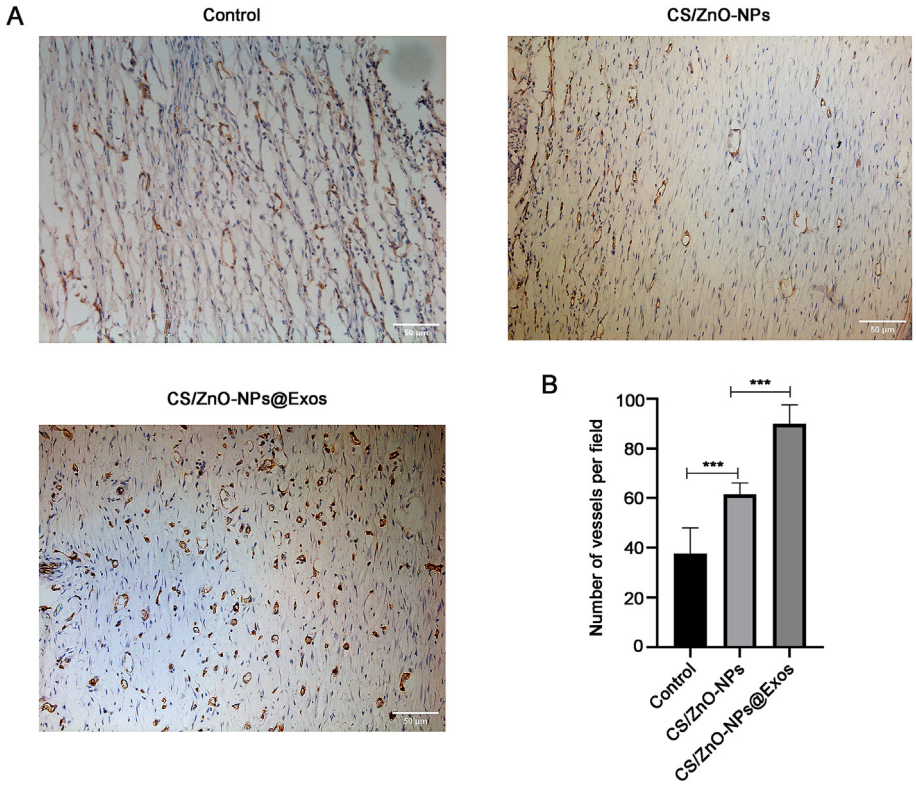

Fig. 5. IHC study for the expression of CD31 was performed to assess angiogenesis in the wounds. (A) Representative images of immunohistochemical staining of CD31 in wound beds at 14 days after surgery. Scale bar, 50 μm. (B) Quantitative analysis of the number of new blood vessel per field (n = 6). ***$P < 0.001$.

elastin, while also releasing various growth factors that regulate cell proliferation and differentiation [44]. Consequently, the effect of H-Exos on the biological characteristics of HFF-1 cells was first observed in this study. Our results demonstrate that H-Exos are efficiently internalized by HFF-1 cells and significantly promote cell migration and proliferation. These findings provide a foundation for future research aimed at developing H-Exos-based composite gels and further exploring their potential for tissue repair in DFUs.

Despite the positive role of Exos in wound repair, their application alone still faces challenges such as poor stability and difficulties in controlled release. Appropriate wound dressings can significantly enhance wound closure. Study has indicated that combining Exos secreted by synovial mesenchymal stem cells with CS hydrogel can notably promote angiogenesis and re-epithelialization at the wound area [45]. Furthermore, Shi et al. demonstrated that loading Exos into porous gel sponge dressings made of CS and silk fibroin, both of which exhibit good biocompatibility, also can effectively promote re-epithelialization, collagen deposition, and angiogenesis [46]. Therefore, the therapeutic approach combining Exos with hydrogel dressings has shown superior efficacy in wound repair.

It has been reported in several studies that CS, when utilized as a wound dressing, can achieve controlled, localized, and sustained release through its interaction with Exos [47]. ZnO-NPs, a novel class of inorganic nanomaterials, possess exceptional antibacterial properties, a lack of resistance development, and favorable biocompatibility. Studies have demonstrated that the incorporation of ZnO-NPs significantly enhances antimicrobial efficacy against pathogenic microorganisms including Escherichia coli, Staphylococcus aureus, and Pseudomonas aeruginosa, with the antibacterial activity showing concentration-dependent characteristics [23,48,49]. The synergistic effect between CS and ZnO-NPs contributes to bacterial membrane disruption and biofilm inhibition [50]. In clinical practice, more than half of DFUs patients are complicated by infection [18]. Therefore, CS/ZnO-NPs composite hydrogels show unique advantages due to their pronounced antibacterial characteristics. The average gelation time of the CS and β-GP hydrogel was 2.49 min. Upon incorporation of ZnO-NPs at concentrations of 1 %, 2 %, and 3 %, the average gelation time was significantly reduced to 1.85, 1.68, and 1.50 min, respectively (data not shown). These results clearly demonstrate that the introduction of ZnO-NPs effectively accelerates gelation at 37 °C. This finding is consistent with previous literature reports [23]. The CS/ZnO-NPs hydrogel prepared in this study exhibits favorable thermosensitivity and injectability, with no significant impact on the proliferation of HFF-1 cells and no observed cytotoxicity, consistent with previous reports. When H-Exos were encapsulated in the CS/ZnO-NPs hydrogel, resulting in the formation of CS/ZnO-NPs@Exos composite hydrogel, a significant enhancement in HFF-1 cell proliferation was observed. These results suggest that the CS/ZnO-NPs@Exos composite hydrogel prepared by this study ensures experimental validity through two distinct mechanisms: first, by maintaining controlled release of Exos to ensure sustained therapeutic action at the wound site; second, through the excellent wound-healing properties conferred by the CS and ZnO-NPs components within the hydrogel matrix, which is consistent with other articles [51]. Collectively, these findings demonstrate that, compared with using Exos alone, the combination of Exos with hydrogels has more application potential and can significantly improve the wound treatment effect.

Fig. 2A shows that H-Exos can be internalized by HFF-1. However, it has not yet been confirmed whether H-Exos can be taken by cells in the local wound tissue. To address this, we applied fluorescently labeled Exos topically and observed that they were similarly internalized by cells at the wound site (Fig. 3G). This

provides experimental evidence supporting the potential role of H-Exos in wound healing.

The difficult healing of DFUs may be attributed to microangiopathy and fibroblast dysfunction leading to limited granulation tissue formation [52]. At the same time, hyperglycemia can impair wound healing by reducing collagen synthesis, triggering structural abnormalities in collagen fibers, and disrupting the temporal sequence of collagen deposition [53]. Both the formation of granulation tissue and the deposition of collagen play critical roles in the wound repair process.

This study evaluated tissue regeneration using HE and Masson staining. The results revealed that, compared to the negative control group, the CS/ZnO-NPs hydrogel treatment group showed no obvious swelling or infection in the local wound, with fewer inflammatory cell infiltrates, accelerated wound healing, and and effectively enhanced re-epithelialization, as well as promoted granulation tissue formation (Fig. 4A–D). More notably, the treatment group using CS/ZnO-NPs@Exos hydrogel showed the most pronounced degree of re-epithelialization, while also facilitating the formation of skin appendages, and achieved the maximum wound healing rate. Wound healing not only relies on granulation tissue formation but also requires collagen deposition [54]. Collagen is a critical component of the extracellular matrix and plays a pivotal role during the proliferation and remodeling stages. The Masson staining results revealed that, compared to the control group, both the CS/ZnO-NPs hydrogel and CS/ZnO-NPs@Exos hydrogel significantly enhanced the deposition of collagen fibers at the wound site, with the CS/ZnO-NPs@Exos hydrogel exhibiting the most remarkable effect (Fig. 4D).

Angiogenesis is a critical process in wound healing, and diabetes mellitus significantly impairs the formation of new blood vessels. In addition, DFUs often involve deep wounds that extend into the subcutaneous tissue, resulting in a frequent deficiency of nutrient supply to the affected areas. HUVECs serve as an ideal cellular model for studying the vascular system and related diseases, as they retain the genetic characteristics of endothelial cells. Furthermore, the abundant secretion of bioactive factors by HUVECs has been shown to effectively promote angiogenesis [55]. Based on these observations, we hypothesize that Exos secreted by HUVECs may possess similar pro-angiogenic properties. This study evaluates angiogenesis by observing CD31 immunohistochemical staining in the injured area and quantifying microvascular density to assess the extent of angiogenesis. Compared to the control group, experimental data indicated that both the CS/ZnO-NPs hydrogel group and the CS/ZnO-NPs@Exos hydrogel group exhibited an increase in angiogenesis. Especially in CS/ZnO-NPs@Exos hydrogel group, the number of blood vessels was the largest and most of the blood vessels showed a well-formed lumen structure. These observations may help to explain why the CS/ZnO-NPs hydrogel loaded with H-Exos is capable of accelerating diabetic wound closure. However, the specific mechanism by which CS/ZnO-NPs@Exos hydrogel promotes wound healing was not thoroughly explored in this study. Future research will aim to further explore the mechanisms of H-Exos action, particularly by utilizing RNA sequencing or mass spectrometry to identify the specific RNA molecules or proteins in H-Exos that play a pivotal role in the wound healing process, and how these molecules activate relevant signaling pathways to promote wound repair.

Based on the above findings, this study indicates that CS/ZnO-NPs@Exos hydrogel, as a bioactive ingredient-containing dressing, can accelerate wound healing by promoting re-epithelialization, collagen deposition, and angiogenesis. It exhibits significant potential in enhancing skin wound repair and tissue regeneration. Future research should further explore the mechanism of action of H-Exos combined with CS/ZnO-NPs hydrogel in skin repair, with the aim of improving its reliability and efficacy in clinical applications.

5. Conclusion

In this study, we demonstrated that CS/ZnO-NPs hydrogels loaded with H-Exos can serve as efficient bioactive wound dressings by providing the sustained release of H-Exos to promote skin ulcer wound healing. Our results indicate that the combination of CS/ZnO-NPs hydrogels and Exos can enhance the bioactivity of the Exos. The CS/ZnO-NPs@Exos hydrogel positively affects wound healing by promoting wound re-epithelialization and collagen deposition and stimulating angiogenesis. These findings suggest that the combination of Exos and a biocompatible wound dressing scaffold holds promise as a novel cell-free therapy for skin tissue repair and regeneration.

Consent to participate

Not applicable.

Ethics approval

S20240412-004.

Consent for publication

All authors have read and agreed to the submitted version of the manuscript.

Data availability statement

All datasets generated for this study are included in the article/Supplementary Material.

Authors' contributions

All authors contributed to the study. All authors were involved in literature search and writing of the manuscript.

Funding

This work was supported by following funds:

1. Nantong University Affiliated Hospital Research-Oriented Hospital Construction Fund ‘Champion the Best’ — Research-Oriented Discipline (Joint) Development Fund (YJXYY202204-XKB09).

2. The Science and Technology plan projects of Nantong Grant (No. MSZ2023155, No. MS22019005, No. JCZ2023004, No. MS22022021).

3. Standardized Diagnosis and Treatment of Endocrine Hypertension (LCYJ-A07).

4. A Clinical Intervention Study of Tangningtongluo on Diabetic Foot Ulcer (HXKT20211001).

Declaration of competing interest

The authors declare that they have no known competing financial interests or personal relationships that could have appeared to influence the work reported in this paper.

Yunjuan Gu reports equipment, drugs, or supplies was provided by Nantong Xingzhong Cell Engineering Co. LTD. Yunjuan Gu reports equipment, drugs, or supplies was provided by Affiliated Hospital of Nantong University. If there are other authors, they declare that they have no known competing financial interests or

personal relationships that could have appeared to influence the work reported in this paper.

Appendix A. Supplementary data

Supplementary data to this article can be found online at https://doi.org/10.1016/j.reth.2025.04.020.

References

[1] Armstrong DG, Boulton AJM, Bus SA. Diabetic foot ulcers and their recurrence. N Engl J Med 2017;376(24):2367–75.
[2] Cho NH, Shaw JE, Karuranga S, Huang Y, da Rocha Fernandes, Ohlrogge., et al. IDF Diabetes Atlas: global estimates of diabetes prevalence for 2017 and projections for 2045. Diabetes Res Clin Pract 2018;138:271–81.
[3] Rodriguez-Rodriguez N, Martínez-Jiménez I, García-Ojalvo A, Mendoza-Mari Y, Guillén-Nieto G, Armstrong DG, et al. Wound chronicity, impaired immunity and infection in diabetic patients. MEDICC Rev 2022;24(1):44–58.
[4] Ahmed AS, Antonsen EL. Immune and vascular dysfunction in diabetic wound healing. J Wound Care 2016;25(Sup7):S35–46.
[5] Lim JZ, Ng NS, Thomas C. Prevention and treatment of diabetic foot ulcers. J R Soc Med 2017;110(3):104–9.
[6] Yang J, Chen Z, Pan D, Li H, Shen J. Umbilical cord-derived mesenchymal stem cell-derived exosomes combined pluronic F127 hydrogel promote chronic diabetic wound healing and complete skin regeneration. Int J Nanomed 2020;15:5911–26.
[7] Bakadia BM, Qaed Ahmed AA, Lamboni L, Shi Z, Mutu Mukole B, Zheng R, et al. Engineering homologous platelet-rich plasma, platelet-rich plasma-derived exosomes, and mesenchymal stem cell-derived exosomes-based dual-crosslinked hydrogels as bioactive diabetic wound dressings. Bioact Mater 2023;28:74–94.
[8] Zhou Y, Zhao B, Zhang XL, Lu YJ, Lu ST, Cheng J, et al. Combined topical and systemic administration with human adipose-derived mesenchymal stem cells (hADSC) and hADSC-derived exosomes markedly promoted cutaneous wound healing and regeneration. Stem Cell Res Ther 2021;12(1):257.
[9] Zhang Y, Li M, Wang Y, Han F, Shen K, Luo L, et al. Exosome/metformin-loaded self-healing conductive hydrogel rescues microvascular dysfunction and promotes chronic diabetic wound healing by inhibiting mitochondrial fission. Bioact Mater 2023;26:323–36.
[10] Song Y, You Y, Xu X, Lu J, Huang X, Zhang J, et al. Adipose-derived mesenchymal stem cell-derived exosomes biopotentiated extracellular matrix hydrogels accelerate diabetic wound healing and skin regeneration. Adv Sci (Weinh) 2023;10(30):e2304023.
[11] Hu P, Yang Q, Wang Q, Shi C, Wang D, Armato U, et al. Mesenchymal stromal cells-exosomes: a promising cell-free therapeutic tool for wound healing and cutaneous regeneration. Burns Trauma 2019;7:38.
[12] Rackov G, Garcia-Romero N, Esteban-Rubio S, Carrión-Navarro J, Belda-Iniesta C, Ayuso-Sacido A. Vesicle-mediated control of cell function: the role of extracellular matrix and microenvironment. Front Physiol 2018;9:651.
[13] Kalluri R, LeBleu VS. The biology, function, and biomedical applications of exosomes. Science 2020;367(6478).
[14] Li D, Wu N. Mechanism and application of exosomes in the wound healing process in diabetes mellitus. Diabetes Res Clin Pract 2022;187:109882.
[15] Yamaguchi H, Ishii E, Tashiro K, Miyazaki S. Role of umbilical vein endothelial cells in hematopoiesis. Leuk Lymphoma 1998;31(1–2):61–9.
[16] Yildirim S, Boehmler AM, Kanz L, Möhle R. Expansion of cord blood CD34+ hematopoietic progenitor cells in coculture with autologous umbilical vein endothelial cells (HUVEC) is superior to cytokine-supplemented liquid culture. Bone Marrow Transplant 2005;36(1):71–9.
[17] Zhao D, Yu Z, Li Y, Wang Y, Li Q, Han D. GelMA combined with sustained release of HUVECs derived exosomes for promoting cutaneous wound healing and facilitating skin regeneration. J Mol Histol 2020;51(3):251–63.
[18] Prompers L, Huijberts M, Apelqvist J, Jude E, Piaggesi A, Bakker K, et al. High prevalence of ischaemia, infection and serious comorbidity in patients with diabetic foot disease in Europe. Baseline results from the Eurodiale study. Diabetologia 2007;50(1):18–25.
[19] Ju Y, Hu Y, Yang P, Xie X, Fang B. Extracellular vesicle-loaded hydrogels for tissue repair and regeneration. Mater Today Bio 2023;18:100522.
[20] Hu JL, Luo HL, Liu JP, Zuo C, Xu YS, Feng X, et al. Chitosan biomaterial enhances the effect of OECs on the inhibition of sciatic nerve injury-induced neuropathic pain. J Chem Neuroanat 2023;133:102327.
[21] Fan X, Su Z, Zhang W, Huang H, He C, Wu Z, et al. An advanced chitosan based sponges dressing system with antioxidative, immunoregulation, angiogenesis and neurogenesis for promoting diabetic wound healing. Mater Today Bio 2024;29:101361.
[22] Zhang C, Yang X, Hu W, Han X, Fan L, Tao S. Preparation and characterization of carboxymethyl chitosan/collagen peptide/oxidized konjac composite hydrogel. Int J Biol Macromol 2020;149:31–40.
[23] Huang P, Su W, Han R, Lin H, Yang J, Xu L, et al. Physicochemical, antibacterial properties, and compatibility of ZnO-NP/chitosan/beta-glycerophosphate composite hydrogels. J Microbiol Biotechnol 2022;32(4):522–30.
[24] Jahangiri B, Khalaj-Kondori M, Asadollahi E, Purrafee Dizaj L, Sadeghizadeh M. MSC-derived exosomes suppress colorectal cancer cell proliferation and metastasis via miR-100/mTOR/miR-143 pathway. Int J Pharm 2022;627:122214.
[25] Barjasteh M, Dehnavi SM, Ahmadi Seyedkhani S, Akrami M. Cu-vitamin B3 donut-like MOFs incorporated into TEMPO-oxidized bacterial cellulose nanofibers for wound healing. Int J Pharm 2023;646:123484.
[26] Kang S, Shi X, Chen Y, Zhang L, Liu Q, Lin Z, et al. Injectable decellularized Wharton's jelly hydrogel containing CD56(+) umbilical cord mesenchymal stem cell-derived exosomes for meniscus tear healing and cartilage protection. Mater Today Bio 2024;29:101258.
[27] Li X, Xie X, Lian W, Shi R, Han S, Zhang H, et al. Exosomes from adipose-derived stem cells overexpressing Nrf2 accelerate cutaneous wound healing by promoting vascularization in a diabetic foot ulcer rat model. Exp Mol Med 2018;50(4):1–14.
[28] Chen LL, Shi WP, Zhang TD, Zhou YQ, Zhao FZ, Ge WY, et al. Antibacterial activity of lysozyme-loaded cream against MRSA and promotion of scalded wound healing. Int J Pharm 2022;627:122200.
[29] Zha W, Wang J, Guo Z, Zhang Y, Wang Y, Dong S, et al. Efficient delivery of VEGF-A mRNA for promoting diabetic wound healing via ionizable lipid nanoparticles. Int J Pharm 2023;632:122565.
[30] Zhang FX, Liu P, Ding W, Meng QB, Su DH, Zhang QC, et al. Injectable Mussel-Inspired highly adhesive hydrogel with exosomes for endogenous cell recruitment and cartilage defect regeneration. Biomaterials 2021;278:121169.
[31] Banerjee P, Suguna L, Shanthi C. Wound healing activity of a collagen-derived cryptic peptide. Amino Acids 2015;47(2):317–28.
[32] Diegelmann RF, Evans MC. Wound healing: an overview of acute, fibrotic and delayed healing. Front Biosci 2004;9:283–9.
[33] de Sousa Victor R, Marcelo da Cunha Santos A, Viana de Sousa B, de Araújo Neves G, Navarro de Lima Santana L, Rodrigues Menezes R. A review on chitosan's uses as biomaterial: tissue engineering, drug delivery systems and cancer treatment. Materials (Basel) 2020;13(21).
[34] Ha D, Yang N, Nadithe V. Exosomes as therapeutic drug carriers and delivery vehicles across biological membranes: current perspectives and future challenges. Acta Pharm Sin B 2016;6(4):287–96.
[35] Shabbir A, Cox A, Rodriguez-Menocal L, Salgado M, Van Badiavas E. Mesenchymal stem cell exosomes induce proliferation and migration of normal and chronic wound fibroblasts, and enhance angiogenesis in vitro. Stem Cells Dev 2015;24(14):1635–47.
[36] Ma T, Fu B, Yang X, Xiao Y, Pan M. Adipose mesenchymal stem cell-derived exosomes promote cell proliferation, migration, and inhibit cell apoptosis via Wnt/beta-catenin signaling in cutaneous wound healing. J Cell Biochem 2019;120(6):10847–54.
[37] Yang J, Hu Y, Wang L, Sun X, Yu L, Guo W. Human umbilical vein endothelial cells derived-exosomes promote osteosarcoma cell stemness by activating Notch signaling pathway. Bioengineered 2021;12(2):11007–17.
[38] Li L, Mu J, Zhang Y, Zhang C, Ma T, Chen L, et al. Stimulation by exosomes from hypoxia preconditioned human umbilical vein endothelial cells facilitates mesenchymal stem cells angiogenic function for spinal cord repair. ACS Nano 2022;16(7):10811–23.
[39] Ellistasari EY, Kariosentono H, Purwanto B, Wasita B, Riswiyant RCA, Pamungkasari EP, et al. Exosomes derived from secretome human umbilical vein endothelial cells (Exo-HUVEC) ameliorate the photo-aging of skin fibroblast. Clin Cosmet Investig Dermatol 2022;15:1583–91.
[40] Kapoor KS, Harris K, Arian KA, Ma L, Schueng Zancanela B, Church KA, et al. High throughput and rapid isolation of extracellular vesicles and exosomes with purity using size exclusion liquid chromatography. Bioact Mater 2024;40:683–95.
[41] An M, Wu J, Zhu J, Lubman DM. Comparison of an optimized ultracentrifugation method versus size-exclusion chromatography for isolation of exosomes from human serum. J Proteome Res 2018;17(10):3599–605.
[42] Montecalvo A, Larregina AT, Shufesky WJ, Stolz DB, Sullivan ML, Karlsson JM, et al. Mechanism of transfer of functional microRNAs between mouse dendritic cells via exosomes. Blood 2012;119(3):756–66.
[43] Broughton G, Janis JE, Attinger CE. Wound healing: an overview. Plast Reconstr Surg 2006;117(7 Suppl):1e-S–32e-S.
[44] Voza FA, Huerta CT, Le N, Shao H, Ribieras A, Ortiz Y, et al. Fibroblasts in diabetic foot ulcers. Int J Mol Sci 2024;25(4).
[45] Tao SC, Guo SC, Li M, Ke QF, Guo YP, Zhang CQ. Chitosan wound dressings incorporating exosomes derived from MicroRNA-126-overexpressing synovium mesenchymal stem cells provide sustained release of exosomes and heal full-thickness skin defects in a diabetic rat model. Stem Cells Transl Med 2017;6(3):736–47.
[46] Shi Q, Qian Z, Liu D, Sun J, Wang X, Liu H, et al. GMSC-derived exosomes combined with a chitosan/silk hydrogel sponge accelerates wound healing in a diabetic rat skin defect model. Front Physiol 2017;8:904.
[47] Wu Q, Guo Y, Li H, Zhang D, Wang S, Hou J, et al. Recombinant human collagen I/carboxymethyl chitosan hydrogel loaded with long-term released hUCMSCs derived exosomes promotes skin wound repair. Int J Biol Macromol 2024;265(Pt 1):130843.
[48] Pulit-Prociak J, Staroń A, Staroń P, Chmielowiec-Korzeniowska A, Drabik A, Tymczyna L, et al. Preparation and of PVA-based compositions with embedded silver, copper and zinc oxide nanoparticles and assessment of their antibacterial properties. J Nanobiotechnol 2020;18(1):148.

[49] Ramzan A, Mehmood A, Ashfaq R, Andleeb A, Butt H, Zulfiqar S, et al. Zinc oxide loaded chitosan-elastin-sodium alginate nanocomposite gel using freeze gelation for enhanced adipose stem cell proliferation and antibacterial properties. Int J Biol Macromol 2023;233:123519.
[50] Elmehbad NY, Mohamed NA, Abd El-Ghany NA, Abdel-Aziz MM. Reinforcement of the antimicrobial activity and biofilm inhibition of novel chitosan-based hydrogels utilizing zinc oxide nanoparticles. Int J Biol Macromol 2023;246:125582.
[51] Shi Y, Wang S, Wang K, Yang R, Liu D, Liao H, et al. Relieving macrophage dysfunction by inhibiting SREBP2 activity: a hypoxic mesenchymal stem cells-derived exosomes loaded multifunctional hydrogel for accelerated diabetic wound healing. Small 2024;20(25):e2309276.
[52] Yan L, Wang Y, Feng J, Ni Y, Zhang T, Cao Y, et al. Mechanism and application of fibrous proteins in diabetic wound healing: a literature review. Front Endocrinol (Lausanne) 2024;15:1430543.
[53] Kanta J, Zavadakova A, Sticova E, Dubsky M. Fibronectin in hyperglycaemia and its potential use in the treatment of diabetic foot ulcers: a review. Int Wound J 2023;20(5):1750–61.
[54] Mathew-Steiner SS, Roy S, Sen CK. Collagen in wound healing. Bioengineering (Basel) 2021;8(5).
[55] Luo ML, Liu XP, Wang F, Liu XX, Liu WF, Wu D, et al. Conditioned medium from human umbilical vein endothelial cells promotes proliferation, migration, invasion and angiogenesis of adipose derived stem cells. Curr Med Sci 2018;38(1):124–30.